A Novel High Efficiency and Ultra Stable Red Emitting Europium Doped Pyrophosphate Phosphor for Multifunctional Application

Chuang Wang[1*], Ying Li[1], Shuanglong Chen[1], Yanyan Li[3], Qingyi Lv[1], Bohuai Shao[1], Ge Zhu[1,2*], Lei Zhao[3*]

1. College of Chemistry and Materials Engineering, Bohai University, Jinzhou, 121000, P. R. China

2. Key Laboratory of New Energy and Rare Earth Resource Utilization of State Ethnic Affairs Commission, College of Physics and Materials Engineering, Dalian Minzu University, 18 Liaohe West Road, Dalian, 116600, P. R. China.

3. Collaborative Innovation Center of Rare-Earth Optical Functional Materials and Devices Development, School of Physics and Opto-Electronic Technology, Baoji University of Arts and Sciences, Baoji, 721016, P. R. China.

CONTENTS

1. Synthesis of RBPO: Eu^{3+}

Synthesis

Rb$_2$Ba$_3$(P$_2$O$_7$)$_2$: Eu^{3+}(RBPO) phosphors were synthesized by a high-temperature solid-state reaction with BaCO$_3$ (99%., Aladdin), Rb$_2$CO$_3$(A.R., Aladdin), (NH$_4$)$_2$·HPO$_4$ (99.99%., Aladdin), and Eu$_2$O$_3$ (99.99%, Aladdin) as raw materials. The above stating materials were weighed according to the stoichiometric ratio and then grounded in an agate mortar for 0.5h. The mixtures were grounded and sintered at 750 ^{o}C for 10 h in a muffle furnace. Finally, the as-prepared samples were cooled down to atmospheric temperature for further analysis.

XRD and Rietveld refinement

The XRD patterns were measured by DX-2700BH (Dandong HaoYuan Co. Ltd) with 30 mA and 40 kV. CuKa radiation is used as excitation source with angle range between 10° and 80°. Program GSAS was used to calculate the crystal structure of RBPO: Eu^{3+}.

Luminescence Spectra

An FSL 1000 fluorescence spectrophotometer was employed to examine the photoluminescence spectra and the fluorescence decay times. A 450 W xenon light source was equipped on a fluorescence spectrophotometer. The PL spectrum dependent on the temperature was investigated by a heat booster (TCB1402C) equipped on a fluorescence spectrophotometer. The internal quantum efficiency values were measured using the integrated sphere on the same FLS1000 instrument. The temperature dependent spectra were measured by a self-built platform for in situ UV-Vis absorption and fluorescence measurement equipped with a 360 nm laser source under high pressure with a modified spectrophotometer (Ocean Optics, QE65 Pro) A modified Mp-Micro-S instrument was used to obtain the cathodoluminescence (CL) properties.

SEM, TEM and EDS

The elemental analysis and morphology were performed using a Hitachi S-4800 equipped with an energy-dispersive spectroscopy (EDS) detector. The morphology and selective area electron diffraction (SAED) pattern were confirmed by the transmission electron microscope (TEM) (FEI Tacnai F30).

Fabrication of LEDs and films

The photoelectric properties of the LED were measured by using an integrating sphere spectroradiometer system (HS-885, HangZhou Starspec optoelectronic Technology). For the PDMS film, the starting materials include base resin and curing agent (Dow Corning Co). At first, 2.5 g base resin, 0.25 g curing agent, and the phosphor were weighted and uniformly stirred for 15 min. Later, the vacuum desiccator (HT-VD008) was used to remove trapped air by 5 min. After that, the mixed powder slurry was dried in an oven at the temperature of 80 ^{o}C for 1 h.

Raman spectra

The Raman spectra were measured by Jobin-Yvon HR 800 pumped by a 785 nm laser source. A special miniature diamond anvil cell (DAC) was used to generate pressures up to nearly 20 GPa at room temperature. A mixture of methanol/ethanol was used as the pressure transmitting medium. The pressure and the hydrostatic conditions experienced by the sample were determined by the shift and broadening of the ruby R1 lines

Fourier transform infrared spectroscopy

Fourier transform infrared spectroscopy (FTIR) was conducted by the standard KBr pellet method on a IRTracer-100 instrument (SHIMADZU, Tokyo).

2. Structure analysis of RBPO: xEu^{3+} (x = 1%, 3%, 5%, 7%, and 10%)

Table S1. Atomic coordinates and equivalent isotropic displacement parameters for BRPO

| Atom	Wyck.	frac	x	y	z	U_{iso}
Ba1	4a	1	0.9347(1)	0.9451(3)	0.8745(8)	0.0096(2)
Ba2	4a	1	0.2548(8)	0.3340(3)	0.8379(9)	0.0071(3)
Ba3	4a	1	0.9228(6)	0.5201(1)	0.5056(7)	0.0184(3)
Rb1	4a	1	0.5834(1)	0.2980(1)	0.6275(1)	0.0106(6)
Rb2	4a	1	0.7739(1)	0.1769(2)	0.8299(1)	0.0171(8)
P1	4a	1	0.2901(1)	0.4064(1)	0.5124(8)	0.0077(9)
P2	4a	1	0.5278(1)	0.6225(1)	0.5143(8)	0.0067(2)
P3	4a	1	0.6151(1)	0.5459(1)	0.7936(7)	0.0082(3)
P4	4a	1	0.8867(1)	0.4553(2)	0.7093(9)	0.0068(4)
O1	4a	1	0.2297(1)	0.4541(1)	0.4377(1)	0.0151(2)
O2	4a	1	0.1659(1)	0.3918(3)	0.5683(6)	0.0132(3)
O3	4a	1	0.3918(2)	0.2768(1)	0.5056(5)	0.0134(3)
O4	4a	1	0.3833(3)	0.5401(2)	0.5472(4)	0.0096(8)
O5	4a	1	0.4829(4)	0.6794(3)	0.4414(2)	0.0161(6)
O6	4a	1	0.5545(1)	0.7411(1)	0.5682(1)	0.0146(9)
O7	4a	1	0.3646(6)	0.4637(3)	0.3081(6)	0.0124(2)
O8	4a	1	0.4827(9)	0.5370(4)	0.7542(7)	0.0128(1)
O9	4a	1	0.6784(1)	0.6957(1)	0.7841(8)	0.0139(3)
O10	4a	1	0.6445(1)	0.4940(9)	0.8692(1)	0.0140(3)
O11	4a	1	0.7173(3)	0.4451(8)	0.7414(2)	0.0130(2)
O12	4a	1	0.8929(4)	0.5812(7)	0.6590(1)	0.0167(2)
O13	4a	1	0.9513(8)	0.4790(6)	0.7779(9)	0.0219(1)
O14	4a	1	0.8974(7)	0.3143(1)	0.6713(4)	0.0219(2)
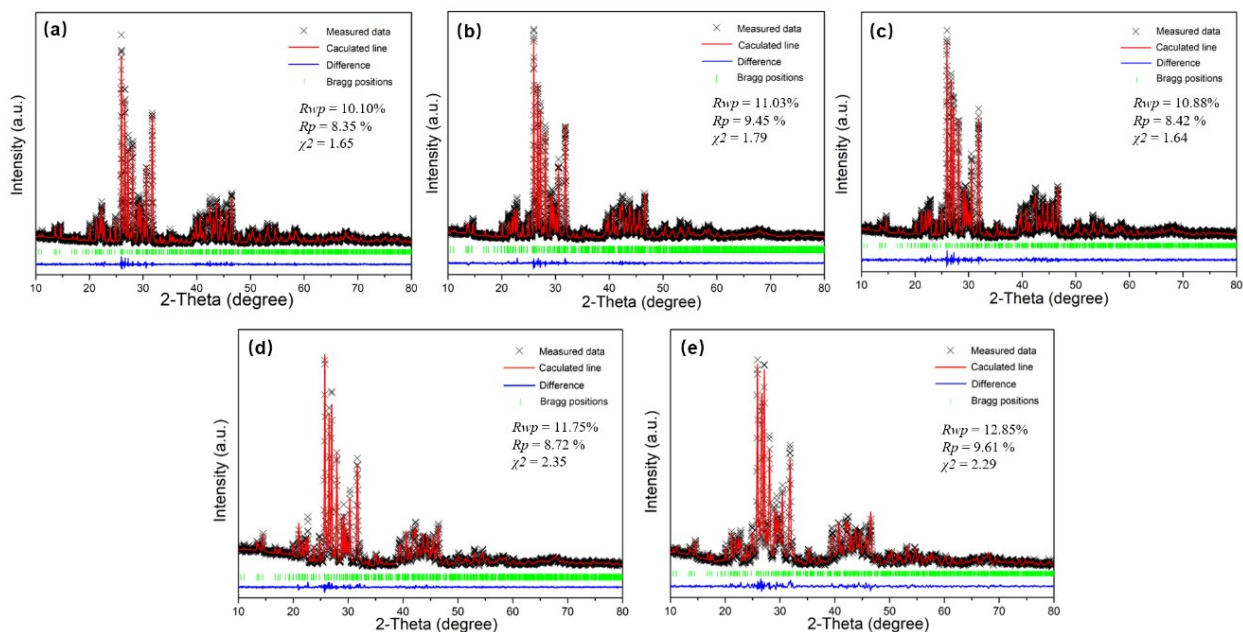
Fig. S1 Rietveld refinement results of RBPO: xEu^{3+} (x = 1%, 3%, 5%, 7%, and 10%)

Table S2. Detailed bond length of Ba-O and Rb-O.

| Bond length (Å)		Bond length (Å)		Bond length (Å)		Bond length (Å)		Bond length (Å)	
Ba1-O2	2.6224	Ba2-O1	2.7031	Ba3-O1	3.0031	Rb1-O1	2.9639	Rb2-O2	3.3173
Ba1-O3	2.9005	Ba2-O5	2.8399	Ba3-O2	2.6331	Rb1-O3	2.8334	Rb2-O4	2.9606
Ba1-O7	2.7615	Ba2-O6	2.6788	Ba3-O3	2.9045	Rb1-O4	3.2536	Rb2-O5	3.2838
Ba1-O9	2.8893	Ba2-O8	2.8327	Ba3-O5	2.9311	Rb1-O7	2.9914	Rb2-O6	3.5395
Ba1-O10	2.8087	Ba2-O9	2.6790	Ba3-O6	2.8079	Rb1-O8	3.2016	Rb2-O8	3.0828
Ba1-O13	2.7071	Ba2-O12	2.7457	Ba3-O7	2.5906	Rb1-O8	3.5739	Rb2-O10	3.2812
Ba1-O14	2.6697	Ba2-O13	2.8188	Ba3-O10	2.6994	Rb1-O9	3.0111	Rb2-O11	3.0469
				Ba3-O12	2.8290	Rb1-O10	3.5134	Rb2-O12	3.1211
						Rb1-O11	2.7847	Rb2-O13	3.4437
						Rb1-O14	2.9274	Rb2-O13	3.5262
								Rb2-O14	3.3814
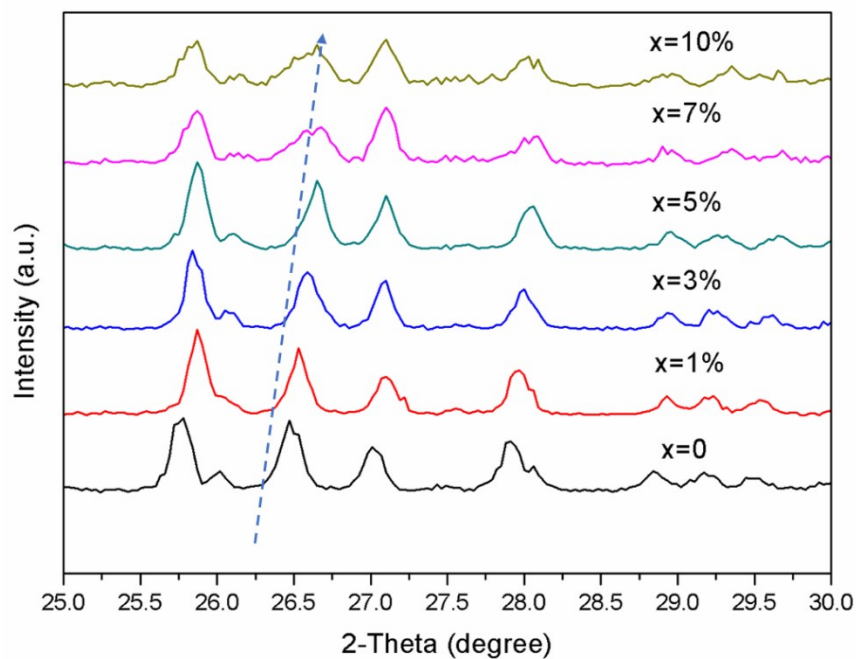
Fig. S2 Enlarged XRD patterns of RBPO: xEu^{3+} (x = 0, 1%, 3%, 5%, 7%, and 10%)
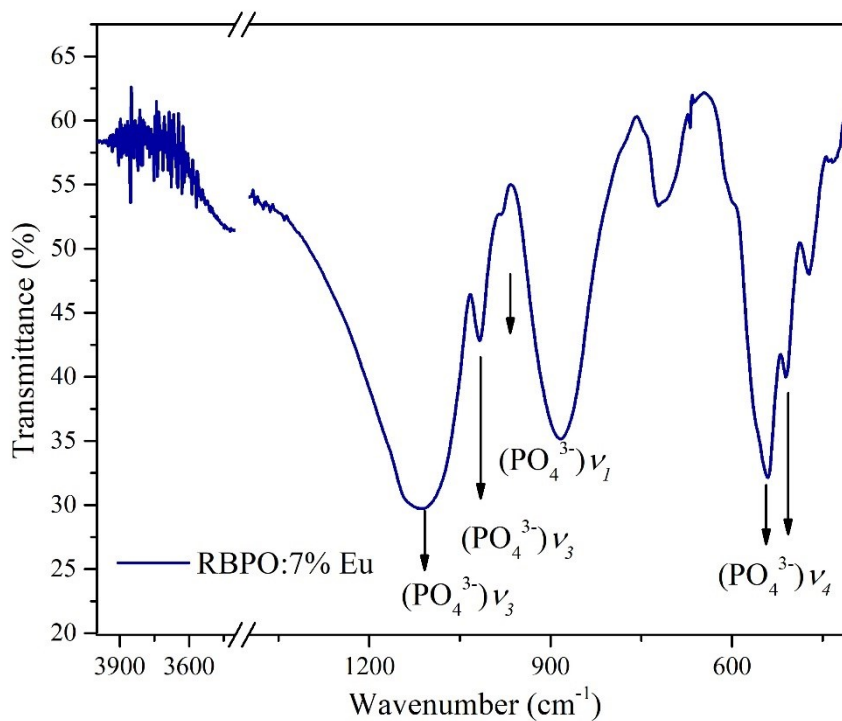
3. Fourier-transform infra-red (FT-IR) spectroscopy

Fig. S3 The FT-IR spectrum of RBPO: $7\%Eu^{3+}$
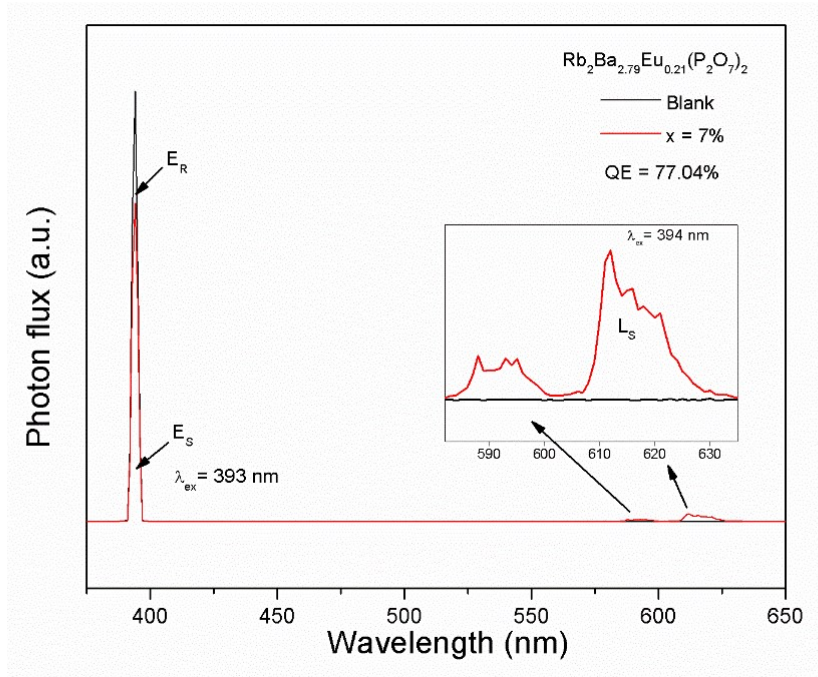
4. Internal quantum efficiency of RBPO: 7%Eu^{3+}

Fig. S4 Excitation lines of BaSO$_4$ and the emission spectrum of RBPO: 7%Eu^{3+} excited by 393 nm collected by using an integrating sphere. The inset shows a magnification of the emission spectrum.

Internal (η_i) quantum efficiencies (QEs) were calculated by using the following equations: [1]

$$\eta_i = \frac{\varepsilon}{\alpha} = \frac{\int L_S}{\int E_R - \int E_S}$$

where ε is the number of photons emitted by the sample and α is the number of photons absorbed by the sample. L_S is the luminescence emission spectrum of the sample; E_R is the spectrum of the excitation light with BaSO$_4$ in the sphere; E_S is the spectrum of the excitation light with the sample in the sphere; and all the spectra were collected using the sphere.

5. PL spectra of RBPO: 7%Eu^{3+} with different charge compensation
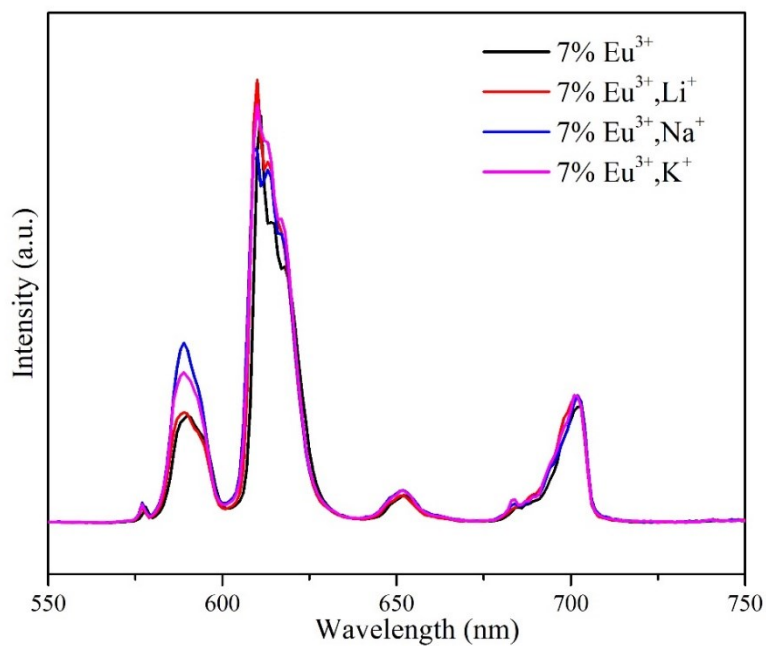

Fig. S5 PL spectra of charge compensated (Li/Na/K)
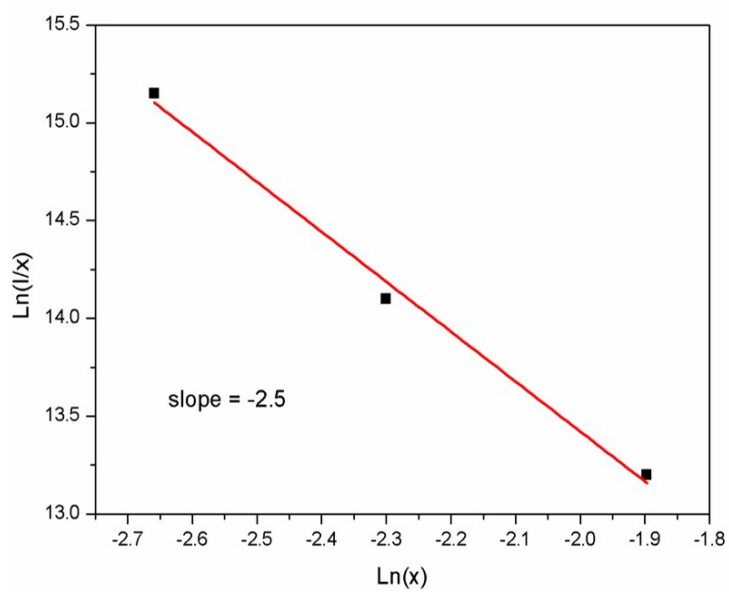
6. Linear fitting of lg(I/x)/lgx for RBPO: xEu^{3+}

Fig. S6 Linear fitting of lg(I/x)/lgx for RBPO: xEu^{3+}

Table S3 Fitting parameters of different decay curves for RBPO:xEu^{3+} (1%≤ x ≤ 10%)

Samples	$A1$	$\tau 1$(μs)	$A2$	$\tau 2$(μs)	t(μs)
x = 1%	736.87	1358.38	838.62	2523.32	2149.23
x = 3%	1171.52	1365.83	1351.11	2442.58	2090.98
x = 5%	550.57	1239.75	1054.56	2279.49	2049.54
x = 7%	517.44	1360.18	866.21	2277.71	2036.46
x = 10%	272.16	1481.52	362.21	2294.9	2029.22

7. The change of I_R (2/1) depended on increasing pressure
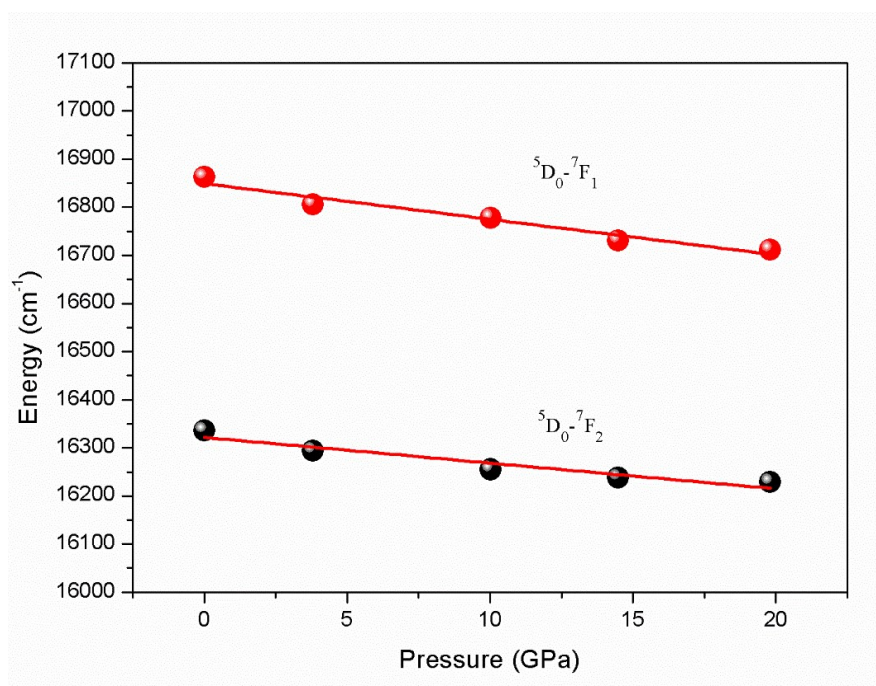
Fig. S7 Peak positions of the $^5D_0 \rightarrow ^7F_1$ and $^5D_0 \rightarrow ^7F_2$ transitions of the Eu^{3+} ions in RBPO: 7%Eu^{3+} as a function of pressure.
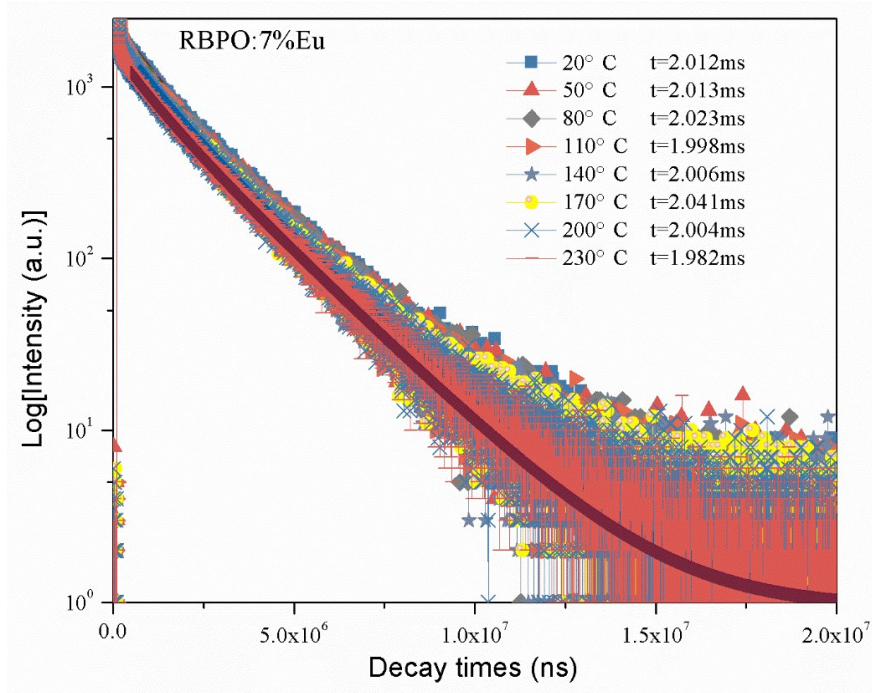
8. The lifetimes depended on increasing temperature

Fig. S8 Temperature dependent lifetimes of RBPO: 7%Eu^{3+}

9. Color purity of RBPO: 7%Eu^{3+}

We calculated the color purity of RBPO: 7%Eu^{3+} using the following equation: [2, 3]

$$\text{Color purity} = \frac{\sqrt{(xs - xi)^2 - (ys - yi)^2}}{\sqrt{(xd - xi)^2 - (yd - yi)^2}} \times 100\% \qquad (6)$$

where (x_d, y_d) is the chromaticity coordinate of the dominant wavelength. The dominant wavelength of a color is the single monochromatic wavelength of the spectrum whose chromaticity is on the same straight line as the sample point (x_s, y_s), and the value of (x_i, y_i) is (0.3101, 0.3162). With calculated data above, the color purity of RBPO: 7%Eu^{3+} can reach 96.37%.

10. Arrhenius equation

$$I(T)=I_0[1 + A\ exp(-\Delta E/kT)]^{-1}$$

where I and I_0 refer to the emission intensity measured at the initial and testing temperature T, respectively. ΔE corresponds to the activation energy for thermal quenching, k represents the Boltzmann's constant, and A is also a constant.[4]
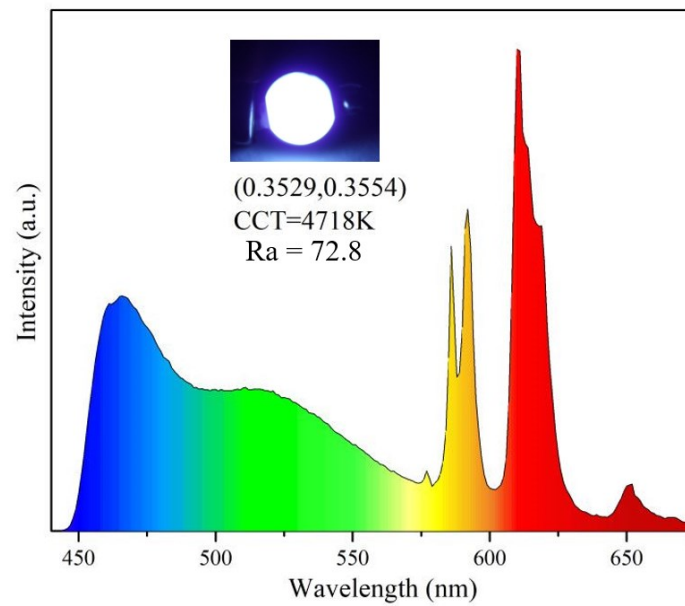

Fig. S9 EL spectrum of the fabricated WLED lamp with 395 nm near-UV LED chip and BAM:Eu2+ blue-emitting phosphors, $(Ba, Sr)_2SiO_4:Eu^{2+}$ green-emitting phosphors, and RBPO:7%Eu^{3+} red-emitting phosphors.

11. Comparative data with other Eu^{3+} doped phosphates phosphors

Table S4 Quantum efficiency, color purity and CIE chromaticity coordinate of the Eu^{3+} doped different phosphates phosphors.

Sample	Quantum Efficiency	Color Purity	CIE Chromaticity Coordinate	Note
$CaTi_4(PO_4)_6:Eu^{3+}$			(0.548, 0.452)	[5]
$CaZn_2(PO_4)_2:Eu^{3+}$	48.79%	100.0%	(0.608, 0.392)	[6]
$Ca_3(PO_4)_2:Eu^{3+}$			(0.578, 0.284)	[7]
$Ca_{10}Li(PO_4)_7:Eu^{3+}$	75.0%		(0.638, 0.361)	[8]
$Sr_3Y(PO_4)_3:Eu^{3+}$	75.0%		(0.640, 0.330)	[9]
$Ca_9Y(PO_4)_7:Eu^{3+}$			(0.650, 0.349)	[10]
$Sr_9LiMg(PO_4)_7:Eu^{3+}$	42.8%	98.4%	(0.650, 0.344)	[11]
$Rb_2Bi(PO_4)(WO_4):Eu^{3+}$		91.0%	(0.648, 0.352)	[12]
$Ca_3La_7(SiO_4)_5(PO_4)O_2:Eu^{3+}$		99.6%	(0.422, 0.529)	[13]
$Ca_3Bi(PO_4)_3:Eu^{3+}$		99.0%	(0.642, 0.358)	[14]
$Sr_9Mg_{1.5}(PO_4)_7:Eu^{3+}$	17.8%		(0.655, 0.345)	[15]
$LiZnPO_4:Eu^{3+}$			(0.490, 0.300)	[16]
$Na_3Gd(PO_4)_2:Eu^{3+}$			(0.630, 0.330)	[17]
$NaZnPO_4:Eu^{3+}$			(0.620, 0.380)	[18]
$Na_{3.6}Y_{1.8}(PO_4)_3:Eu^{3+}$			(0.335, 0.350)	[19]
$NaBaBi_2(PO_4)_3:Eu^{3+}$		88.0%	(0.617, 0.381)	[20]
$Pb_3Bi(PO_4)_3:Eu^{3+}$			(0.620, 0.379)	[21]
$Rb_2Ba_3(P_2O_7)_2:Eu^{3+}$	77.04%	96.4%	(0.647, 0.348)	This Work

12. Reference

[1]   K. Ohkubo and T. Shigeta, Absolute fluorescence quantum efficiency of nbs phosphor standard samples, *J. Illum. Engng. Inst. Jpn.,* 83 (1999**)** 87–93.

[2]   P. Du, X.Y. Huang and J.S. Yu, Facile synthesis of bifunctional Eu^{3+}-activated $NaBiF_4$ red-emitting nanoparticles for simultaneous white light-emitting diodes and field emission displays, *Chem. Eng. J.,* 2018, **337**, 91–100.

[3]   R. Chatterjee, S. Saha, D. Sen, K. Panigrahi, U.K. Ghorai, G.C. Das and K.K. Chattopadhyay, Neutralizing the Charge Imbalance Problem in Eu^{3+}-Activated $BaAl_2O_4$ Nanophosphors:

Theoretical Insights and Experimental Validation Considering K^+ Codoping, *ACS. Omega.,* 2018, **3**, 788–800.

[4] W.H. Fonger and C.W. Struck, Eu^{+3} ^5D Resonance Quenching to the Charge-Transfer States in Y_2O_2S, La_2O_2S, and LaOCl, *J. Chem. Phys.,* 1970, **52**, 6364.

[5] R.P. Cao, W.H. Shao, Y.S. Zhao, T. Chen, H. Ao, S.L. Guo, P. Liu and T. Fan, Orange-red-emitting $CaTi_4(PO_4)_6$: Eu^{3+} phosphor for white LEDs: synthesis and luminescence properties, *Appl. Phys. A.,* 2020, **126**, 267.

[6] T. Krishnapriya, A. Jose, T.A. Jose, E. Sreeja, N.V. Unnikrishnan and P.R. Biju, *J. Mater. Sci.,* 2020, **31**, 22452–22466.

[7] X.G. Zhang, L.Y. Zhou and M.L. Gong, High-brightness Eu^{3+}-doped $Ca_3(PO_4)_2$ red phosphor for NUV light-emitting diodes application, *Opt. Mater.,* 2013, **35**, 993–997.

[8] E.H. Song, W.R. Zhao, G.X. Zhou, X.H. Dou, C.Y. Yi and M.K. Zhou, Luminescence properties of red phosphors $Ca_{10}Li(PO_4)_7$: Eu^{3+}, *J. Rare Earths.,* 2011, **29**, 440-443.

[9] B.Z. Yang, Z.P. Yang, Y.F. Liu, F.C. Lu, P.L. Li, Y.M. Yang and X. Li, Synthesis and photoluminescence properties of the high-brightness Eu^{3+}-doped $Sr_3Y(PO_4)_3$ red phosphors, *Ceram. Int.,* 2012, **38**, 4895–4900.

[10] B.L. Wang, Y.T. Lin and H.D. Ju, Luminescence properties of red-emitting $Ca_9Y(PO_4)_7$: Eu^{3+} phosphor for NUV white-LEDs, *J. Alloys. Comp.,* 2014, **584**, 167–170.

[11] J.B. Luo, Z.S. Sun, Z.P. Zhu, X.G. Zhang, Z.C. Wu and F.W. Mo, Synthesis, structure and luminescence of a high-purity and thermal-stable $Sr_9LiMg(PO_4)_7$: Eu^{3+} red phosphor, *Ceram. Int.,* 2020, **46**, 11994–12000.

[12] Z. Jia, X.L. Zhang, X.Y. Hua, Y. Dong, H.L. Li, C.Q. Feng, Y.G. Wang and M.J. Xia, Engineering mixed polyanion red-emitting $Rb_2Bi(PO_4)(WO_4)$: Eu^{3+} phosphors with negligible thermal quenching and high quantum yield, *J. Alloys Comp.,* 2020, **844**, 155875.

[13] J. Cheng, J. Zhang, X.T. Bian, Z.Y. Zhai and J. Shi, Photoluminescence properties, Judd-Ofelt analysis, and optical temperature sensing of Eu^{3+}-doped $Ca_3La_7(SiO_4)_5(PO_4)O_2$ luminescent materials, Spectrochim, *Acta, Part. A.,* 2020, **230**, 118057.

[14] M.K. Sahu and M. Jayasimhadri, Conversion of blue emitting thermally stable $Ca_3Bi(PO_4)_3$ host as a color tunable phosphor via energy transfer for luminescent devices, *J. Lumin.,* 2020, **227**, 117570.

[15] W.Z. Sun, Y.L. Jia, T.F. Ma, D. Li, H.F. Li, L.H. Jiang, S. Zhang, J.P. Fu, R. Pang and C.Y. Li, Synthesis and Photoluminescence Properties of a Red-Emitting Phosphor $Sr_9Mg_{1.5}(PO_4)_7$: Eu^{3+}, *Chem. Select.,* 2016, **3**, 462–468.

[16] S.A. Bhat, S.U. Islam, M. Faizan and M. Ikram, Synthesis and Luminescent characteristics of Eu^{3+} doped $LiZnPO_4$ phosphors for white LEDs, *Optik.,* 2019, **181**, 836–841.

[17] T. Chengaiah, B.C. Jamalaiah, L. Rama and Moorthy, Luminescence properties of Eu^{3+}-doped $Na_3Gd(PO_4)_2$ red-emitting nanophosphors for LEDs, *Spectrochim, Acta, Part. A.,* 2014, **133**, 495–500.

[18] H. Pan, X. Li, J.P. Zhang, L. Guan, H.X. Su and F. Teng, Synthesis and luminescent properties of $NaZnPO_4$:Eu^{3+} red phosphors for white LEDs, *Mater. Lett.,* 2015, **155**, 106–108.

[19] U. Farooq, X.Y. Sun, Z. Zhao, R.A. Janjua, C. Gao, R.C. Dai, Z.P. Wang and Z.M. Zhang, Thermally stable $Na_{3.6}Y_{1.8}(PO_4)_3$: Eu^{3+} phosphor, luminescent properties and application in WLEDs, *J. Alloys. Comp.,* 2020, **821**, 153513.

[20] B. Yu, Y.C. Li, R.P. Zhang, H. Li and Y.J. Wang, A novel thermally stable eulytite-type $NaBaBi_2(PO_4)_3$: Eu^{3+} red-emitting phosphor for pc-WLEDs, *J. Alloys. Comp.,* 2021, **852**, 157020.

[21] B. Yu, Y.C. Li, Y.J. Wang and L. Geng, A new eulytite-type $Pb_3Bi(PO_4)_3$: Eu^{3+} red-emitting phosphor: Synthesis, structure and photoluminescence characteristics, *J. Lumin.,* 2020, **220**, 116978.